

Research Progress of Spinel Structure ZnFe₂O₄ Anode Materials for Lithium ion Batteries: A Mini-Review

Guang Yang^{1,*}, Zhirong He¹, Yu zhou², Mengyuan Zhao², Yansheng Shen², Hongyuan Zhao^{2,*}

¹ Guangdong Provincial Key Laboratory of Emergency Test for Dangerous Chemicals, Guangdong Institute of Analysis, Guangzhou 510070, China

² Laboratory for Electrochemistry and Energy Engineering (LEEE), Henan Institute of Science and Technology, Xinxiang 453003, China

*E-mail: fygd21@163.com (G. Yang), hongyuanzhao@126.com (H. Zhao)

Received: 30 May 2020 / Accepted: 23 September 2020 / Published: 31 October 2020

The spinel ZnFe₂O₄ anode material has been garnering attention worldwide due to its unique energy storage properties. In this paper, the research progress of ZnFe₂O₄ anode materials for lithium ion batteries was reviewed. Accordingly, the structure morphology and synthesis techniques were first introduced in detail, and the modification strategies such as morphology control and carbon composite optimization were then summarized. Finally, future research prospects regarding ZnFe₂O₄ anode materials for lithium ion batteries were discussed.

Keywords: Lithium ion batteries; ZnFe₂O₄; Synthesis methods; Morphology control; Carbon composite optimization

1. INTRODUCTION

In the last decades, alternative energy devices and energy storage systems have been constantly developed due to environmental problems caused by fossil fuel combustion. Currently, lithium ion batteries are becoming the most potential energy storage equipment due to their high energy density, long cycle life and no pollution [1-8]. These lithium ion batteries have been widely used in portable electronics, new energy vehicles, smart grids and other energy storage devices.

The electrochemical activities of lithium ion batteries is highly dependent on the many properties of electrode functional materials, which mainly encompass carbon-based, silicon-based, and tin-based alloys and mixed transition metal oxides [9-15]. Among them, anode materials have played a significant role in preparing high-performance energy storage batteries. Commercial lithium ion batteries are generally developed according to graphite electrode, however, the large-scale application of such materials usually suffer from a big challenges owing to their low theoretical capacity (372 mAh/g), low

lithium intercalation potential and poor rate performance of graphite materials. The research and development involving high-performance anode materials has since become a research hotspot [16-18].

Transition metal oxides of metal organic framework are emphatically studied as new electrode materials, such as Fe₂O₃ [19], SnO₂ [20], ZnFe₂O₄ [21], and NiCo₂O₄ [22], which possess numerous advantages in regard to their rich resources, low-cost and high capacity. Among such electrode materials, spinel ZnFe₂O₄ has been acknowledged as a promising electrode materials due to its large specific capacity (1072 mAh/g) [23-29]. Moreover, compared to other transition metal oxides, it possesses obvious advantages like low toxicity, easy preparation and low cost. However, various problems such as poor electronic conductivity, and rapid capacity fade exist, which are mainly attributed to the variation of stress caused by volume expansion, leading to limit the application and development of ZnFe₂O₄ electrode materials [30-38].

In order to promote a more ideal development and application of ZnFe₂O₄, research pertaining to ZnFe₂O₄ as an electrode materials were reviewed in this paper. Structure and synthesis methods were first introduced in detail, followed by modification strategies such as morphology control and carbon composite optimization. Finally, future research prospects of ZnFe₂O₄ as an advanced electrode materials were discussed.

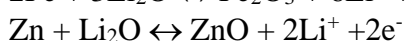
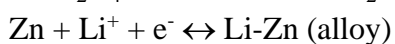
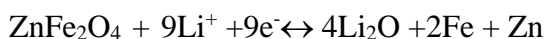
2. STRUCTURE of ZnFe₂O₄

The crystal structure of the ZnFe₂O₄ anode material is forward structure of a typical spinel with a space group of 277(Fd3m). The Zn²⁺ ions preferentially occupy the tetrahedral(A) sites because of their tendency to form covalent bonds involving sp' orbitals, while Fe³⁺ ions are at the octahedral(B) sites in the spinel structure[39-44]. In this regard, Zn²⁺ and Fe³⁺ ions are distributed as (Zn_{1-x}²⁺Fe_x³⁺)[Zn_x²⁺Fe_{2-x}³⁺]O₄ at the (A) and (B) positions.

According to the phase transformation and structure reversible studies in the first charge/discharge process, the Li-Zn alloy and Fe₂O₃ were considered as final products of discharge and recharge, respectively. The mechanism of electrochemical reaction of ZnFe₂O₄ anode material is described as follows. First, 2 mol of Li⁺ are intercalated to form Li₂ZnFe₂O₄. Further intercalation of Li⁺ participating in the conversion reaction may lead to the destruction of spinel ZnFe₂O₄ in order to form Zn, Fe, and the matrix of Li₂O. Then, Li-Zn alloys are formed via alloying reaction. It indicates that a total of 9 lithium ions reacted with ZnFe₂O₄ during the initial discharge.

The charge process is the de-alloying reaction from Li-Zn to Zn metal, where ZnFe₂O₄ cannot be restored. However, Fe₂O₃ and ZnO can be formed through the oxidation reaction of Fe and Zn metals.

The mechanism can be schematized as follows:



3. SYNTHESIS METHODS of ZnFe₂O₄

Recently, several attempts have been made to prepare high-performance ZnFe₂O₄ anode materials by developing a variety of synthesis methods such as solvothermal synthesis, co-precipitation, polymer pyrolysis reaction, electrospinning technology and sol-gel [27, 45-50], as shown in **Table 1**.

3.1 Solvothermal synthesis

Solvothermal synthesis is regarded as a highly versatile way in preparing ZnFe₂O₄ anode materials as well as its composites. Qu et al. [21] reported the facile hydrothermal preparation of porous ZnFe₂O₄ nanospheres material. According to the results of its morphology characterization, the diameter and surface area of porous ZnFe₂O₄ nanospheres are around 200 nm and 37.14 m²/g, respectively. The initial capacity of the fabricated battery is 1098mAh/g at a current density of 200mA/g. Notably, the irreversible capacity of porous ZnFe₂O₄ nanospheres material attains 202 mAh/g, which can be owned to the production of solid electrolyte interphase (SEI) film.

Wang et al. [51] fabricated hollow ZnFe₂O₄ microspheres using a one-step hydrothermal method with carbon ball as a template. The morphology characterization displays that the diameter of hollow ZnFe₂O₄ microspheres was about 300 nm. The electrochemical performance of lithium ion battery based on ZnFe₂O₄ electrode material exhibited the initial discharge specific capacity of 1524 mAh/g at 100 mA/g. After 50 cycles, the reversible capacity remained at 826 mAh/g with a coulombic efficiency of 100%, suggesting excellent cycling performance.

3.2 Co-precipitation

Co-precipitation has been widely used in the preparation of superfine powder with two or more metallic elements. Zhong et al. [48] prepared mesoporous ZnFe₂O₄ nanorods by a simple co-precipitation strategy followed with thermal decomposition. Accordingly, the hydrolyzation of Fe²⁺ and metal ion oxidation may be avoided by adding a small amount of hydrochloric acid and hexamethylene, respectively. The lithium storage properties of mesoporous ZnFe₂O₄ nanorods electrode materials were investigated by galvanostatic charge/discharge cycling, which demonstrated that a high initial discharge specific capacity was 1231 mAh/g, and the reversible specific capacity of 983 mAh/g of this nanorods material can be obtained after 50 cycles. This good cycling stability of ZnFe₂O₄ may be attributed to their mesoporous nanorod structure, which provides more lithium storage space to improve electrochemical performance.

3.3 Electrospinning

Electrospinning is a type of manufacturing technology used for the preparation of special fiber. Qiao et al. [33] successfully developed a simple and general electrospinning technique, collaborating with post-solvothermal methods in preparing composite nanofiber of ZnFe₂O₄-graphene. The results of

surface morphology and specific surface areas illustrated that ZnFe₂O₄ nanofibers with an average diameter of 120 nm and specific surface areas of 106.8 m²/g were wrapped by graphene sheets. After 50 cycles, the specific reversible capacity was maintained at 1000 mAh/g at a current rate of 0.05 C, suggesting the good cycling performance of ZnFe₂O₄-graphene composite. The enhanced electrochemical properties of ZnFe₂O₄/graphene materials were mainly attributed to the interconnected nanofiber, which provides an efficient conductive network and contact area to decrease the internal resistance and improve utilization of the electrode material.

3.4 Other methods

Ding et al. [45] prepared a ZnFe₂O₄ cubic nanoparticle via simple polymer pyrolysis followed by calcination. The obtained ZnFe₂O₄ cubic nanoparticle exhibited good reversibility and stable capacities. An electrochemical test showed that this material may attain 800 mAh/g with a relatively good capacity retention of about 85% following 50 cycles. Moreover, the material demonstrated broad application potential as an electrode material. Cherian et al. [52] prepared a nanocrystalline spinel (Ni_{1-x}Zn_x)Fe₂O₄ (0 ≤ x ≤ 1) via sol-gel auto-combustion, showing that the material possessed an excellent cycle stability.

Table 1. Preparation method of ZnFe₂O₄ and composites materials

Preparation method	Electrochemical Performance (mAh/g)	Capacity retention (%)	Reference
Hydrothermal	933	87 (100 cycles)	[49]
Co-precipitation	1231	86 (50 cycles)	[48]
Template method	1061	106 (100 cycles)	[27]
Polymer pyrolysis	941	85 (50 cycles)	[45]
Electrospinning	1292	77 (30 cycles)	[46]
Electrodeposition	910	97 (200 cycles)	[47]

4. MORPHOLOGY CONTROL

The electrochemical performance of ZnFe₂O₄ is greatly affected by morphology and micro/nanostructures [53-55]. During the charge/discharge cycles, a controllable morphology can provide sufficient room to relieve volume expansion changes, which contributes to the maintenance of material structure stability. Moreover, the nano-sized structure can greatly reduce the transmission pathway of lithium ion, with promoting ion diffusion and enhancing rate performance. In terms of nano-electrode materials with various morphologies, the electrochemical performance was influenced by

special morphologies like mesoporous structure, hollow microspheres, octahedron, nanoparticles, nanorods and nanosheets [10, 13, 56]. Thus, it serves as a practical method to improve the electrochemical performance of lithium ion batteries by preparing the ZnFe_2O_4 electrode material with a controllable morphology.

Guo et al. [42] synthesized hollow ZnFe_2O_4 microspheres with a hierarchical structure composed of phase-pure ZnFe_2O_4 nanoparticles using the hydrothermal technique followed by annealing. The SEM and TEM images confirm that this material consists of hollow spheres with a small diameter of less than $\sim 1 \mu\text{m}$. Moreover, the size and the thickness of hollow sphere particles were about 10-20 nm and 100 nm, respectively. The electrochemical performance of hollow ZnFe_2O_4 microspheres was examined at a constant current of 65 mA/g. Which indicated that the ZnFe_2O_4 electrode delivers an initial discharge capacity of 1200 mAh/g and a reversible specific capacity of 900 mAh/g can be attained after 50 cycles. Its excellent performance very much involves the unique hollow spherical structure of ZnFe_2O_4 .

Xing et al. [57] described a one-step hydrothermal technique used for the preparation of symmetrical and regular nano-octahedral morphology materials (200 nm) without requiring further heat-decomposition. The cycling performance of ZnFe_2O_4 exhibited 730 mAh/g even after 300 cycles at 1000 mA/g. Related studies have pointed out that based on the spinel electrode material can obtain excellent electrochemical performance, which benefit from unique single crystal properties and nano-size effects. Specifically, the single crystal and nano-size effects can increase the uniform delivery of ions and shorten the Li^+ ion transmission pathways, respectively, thereby further optimizing the electrochemical performance. [58].

Research by Zhong et al. [48] shows that the concentration of ethanol has a significant influence on the morphology of ZnFe_2O_4 materials. When the ethanol concentration in the $\text{H}_2\text{C}_2\text{O}_4$ solution is increased from 0%, 50% to 100%, the morphological changes of the resultant ZnFe_2O_4 via massive cluster rods becomes nanorods. The authors speculated that due to the capping ligand mechanism, the radial growth of ZnFe_2O_4 nanorods will gradually be inhibited as the ethanol concentration increases.

Won et al. [59] employed dextrin as a carbon source in preparing ZnFe_2O_4 yolk-shell electrode material through simple spray-drying. The ZnFe_2O_4 electrode material exhibits an initial discharge capacity of 1226 mAh/g at a density of 500 mA/g with an initial coulombic efficiency of 74%. Furthermore, the discharge capacity of the ZnFe_2O_4 electrode materials remained at 862 mAh/g after 200 cycles. The enhanced coulombic efficiency and cycling performance can be attributed to the spray-drying synthetic yolk-shell powders can maintain the structural integrity of metal oxides during the electrochemical performance test.

Gao et al. [60] obtained ZnFe_2O_4 nanoflakes composite material by using ethylene glycol as the medium through a co-precipitation method followed by annealing, indicating that the morphology of $\text{ZnFe}_2\text{O}_4@C$ nanoflakes materials is greatly affected by the refluxing temperature. With a rise in refluxing temperature gradually increase from 140 °C to 200 °C, the morphology of the $\text{ZnFe}_2\text{O}_4@C$ composite material was slowly changed from sphere-like nanoparticles to micro-flowers, and even further separated nanoflakes.

5. ZnFe₂O₄/CARBON MATERIALS

Although ZnFe₂O₄ possesses a high theoretical capacity up to 1072 mAh/g, the cyclability of ZnFe₂O₄-based lithium ion batteries does not meet practical standards. This may possibly be due to unstable structural of the electrode and they suffer from large volume expansion during the charge/discharge cycles, leading to particle pulverization and rapid decline in capacity. Carbon materials are applied as an effective coating matrixes doped to ZnFe₂O₄ electrode materials [61].

In order to improve the performance of ZnFe₂O₄, numerous studies have attempted to develop ZnFe₂O₄-based hybrid materials with stable structures and excellent properties. The mentioned hybrid materials based on ZnFe₂O₄ mainly involve to various carbonaceous materials and composites consisting of ZnFe₂O₄. The composites of ZnFe₂O₄/carbon nanocoating enable the full use of the synergistic effect of the two materials in effectively buffer and lessen the impact of structural collapse caused by volumetric changes. Furthermore, the high activated surface area and high electronic conductivity of the carbon material, which can increase the transmission capacity of ions at the composite electrode interface.

5.1 ZnFe₂O₄/C

Gao et al. [60] obtained the ZnFe₂O₄ nanoflakes composite material by using ethylene glycol as the medium through a co-precipitation method followed by annealing. The results show that the amorphous carbon-coated ZnFe₂O₄ subunits are attributed to the in-situ carbonization of ethylene glycol on the surface of the ZnFe precursor during the calcination treatment. The electrochemical performance of electrodes based on ZnFe₂O₄@C NFs were investigated by charge and discharge test. The ZnFe₂O₄@C NFs composites showed high rate capability and superior cycling stability with initial discharge capacity of 1394.7 mAh/g and 1038.9 mAh/g, respectively. When the current densities increased from 0.2 to 3 A/g, the discharge capacity slightly declined from 1049 to 776 mA·h/g. Even after 1000 cycles, the ZnFe₂O₄@C NFs composites continued to deliver 778.6 mA·h/g. As the surface forms amorphous carbon coating structures that have excellent conductivity, it can greatly improve electron/ion transmission efficiency and further enhances the performance stability of ZnFe₂O₄@C NFs composites.

Thankachan [28] put forward a composites nano-clusters and particles structure of ZnFe₂O₄-C. The morphological and structure features of the composites indicate that ZnFe₂O₄ nanoparticles are dispersed homogeneously onto the Super P LiTM carbon black substrate, where the ZnFe₂O₄-C composites exhibited a higher specific surface area of 63.2 m²/g than that of the pristine ZnFe₂O₄ material (7.80 m²/g). Moreover, the electrochemical performance test of ZnFe₂O₄-C composites illustrated that it may exhibit 681 mAh/g after 100 cycles with a high coulombic efficiency (82%) .

5.2 ZnFe₂O₄/CNT

Sui [62] described a simple method by in-suit high temperature calcination treatment to obtain ZnFe₂O₄ nanoparticles, which can uniformly disperse on the surface of multi-walled carbon nanotubes(MWCTs) to form a special zinc ferrite-carbon nanotubes heterostructure. The

electrochemical performance of MWCNT-ZnFe₂O₄ nanocomposites were investigated by discharge/charge test. MWCNT-ZnFe₂O₄ nanocomposites exhibited 1792 mAh/g at a current density of 60mA/g with high capacity retention rate after 50 cycles. The outstanding electrochemical property was mainly owing to multi-walled carbon nanotubes increase the electronic conductivity of nanoparticles. Additionally, the micro-nano porous structural of multi-walled carbon nanotubes can hold more Li ion during the insertion-extraction process, and the nanoparticles of the ZnFe₂O₄ were anchored on the carbon nanotubes and the inner holes of the CNTs could accommodate the volume change during the charge and discharge procedures and leading to a remarkable cycles stability.

5.3 ZnFe₂O₄/Graphene

Recently, graphene has been touted to be the most promising next generation of energy materials because of the exceptional properties in terms of high current density, high thermal conductivity, chemical structural stability and large specific surface area. Studies have shown that the combination of graphene and ZnFe₂O₄ can produce a two-dimensional layered electrode material, improving the conductivity, specific surface area and electrochemical properties of ZnFe₂O₄.

Dong et al. [63] prepared a three-dimensional mesoporous ZnFe₂O₄-graphene composites by hydrothermal methods, which exhibited excellent electrochemical performance benefit from the synergistic effects between the uniform dispersion of submicron-sized ZnFe₂O₄ spheres and the highly conductive graphene. The mesoporous ZnFe₂O₄-graphene composites had a high specific capacity of 1182 mAh/g cycling at 100 mA/g. While the ZnFe₂O₄-graphene composites were cycled at 500 mA/g for 200 cycles, the reversible capacity gradually stabilized at 970 mAh/g and demonstrated a good cycle capability.

Wang et al. [64] synthesized ZnFe₂O₄-graphene (ZnFe₂O₄/GAs) aerogel composites using the hydrothermal-calcination two-step method. Morphological characterization showed that ZnFe₂O₄ was well-distributed on the graphene aerogels substrate. Due to the synergetic effect of conductive graphene aerogels and the nanostructured ZnFe₂O₄, compared to pristine ZnFe₂O₄ material, the ZnFe₂O₄-graphene aerogel composites demonstrated good electrochemical performance as well as high reversible specific capacity of 1049mAh/g at a current density of 100mA/g over 100 cycles.

5.4 ZnFe₂O₄/metal oxide materials

Recently, lots of research effort are devoted in preparing and constructing the hierarchical mesoporous composites with micro-/nanostructures, the hierarchical mesoporous composites can make full use of the structural features and electrochemical activities of each component leading to obtain better electrochemical performance [65].

Two or more different mixed metal oxides can uniformly form a layered micro/nano composite material, fully utilizing the interaction of different oxides so as to obtain better electrochemical performance during the charge and discharge processes such as ZnO/ZnFeO₄/C, ZnO/ZnCO₂O₄, CoO/CoFe₂O₄ and ZnO/NiO/ZnCo₂O₄. These composites have better energy storage compared to mono-

component metal oxides materials [66-68]. Hou [67] found that they synthesized hierarchical mesoporous ZnO/ZnFe₂O₄ sub-microcubes via a self-sacrifice template route using Prussian blue analogues precursor. Additionally, the ZnFe₂O₄ mono-component material was obtained by selectively chemical etching of the hierarchical ZnO/ZnFe₂O₄ composites. In the bi-component composite material, the uniformly dispersed ZnO and ZnFe₂O₄ are in the cubic structure also enhanced the pristine metal oxides intrinsic electrical conductivity and thus facilitated the transport of Li ions and electronics. Due to the unique structural features, both ZnO/ZnFe₂O₄ and ZnO were also exhibited excellent electrochemical performances as anode electrodes for lithium-ion batteries.

The cycling stability indicated that the hierarchical mesoporous ZnO/ZnFe₂O₄ sub-microcubes demonstrated a superior electrochemical performance as compared to the ZnO sub-microcubes. The first discharge specific capacity of ZnO/ZnFe₂O₄ and ZnFe₂O₄ is 1892 mAh/g and 854 mAh/g at the same rate. Nevertheless, the discharge capacity fading rapidly during the initial 25 cycles for both of the ZnO/ZnFe₂O₄ and ZnFe₂O₄ composites due to the structural adaptation rearrangement of the active material, as they take reacts with electrolyte to form a stable SEI at the electrode interface. In the subsequent cycles, the capacity stabilized at 837mAh/g at 1000mA/g over 200 cycles; as contrast, the ZnFe₂O₄ electrode show a specific capacity of 487 mAh/g under identical conditions. The good cycling stability as well as high rate capability of ZnO/ZnFe₂O₄ composites was achieved through its uniform hybrid ZnO/ZnFe₂O₄ sub-microcubes formation and high-content symbiotic ZnO in the hybrid. These factors facilitated synergistic effect of the mixed metal oxides, preventing the nanophase metal oxides aggregation during following cycles and enhancing electrochemical performance of the ZnO/ZnFe₂O₄ composites.

Ma [68] synthesized the ZnO/ZnFe₂O₄/N-doped C micro-polyhedrons composites via a facile co-precipitation followed by annealing treatment, and studied their electrochemical performance versus Li metal. The ZnO/ZnFe₂O₄/N-doped C composite materials showed a high reversible specific capacity of 1000 mAh/g when cycled after 100 cycles. The porous ZnO/ZnFe₂O₄/N-doped C composite not only enhanced their cycle stability but also promoted a superior rate capability that retained a reversible capacity of 620 mAh/g even at a high current density of 2.0 A/g over 1000 cycles.

Accordingly, the remarkable properties of ZnO/ZnFe₂O₄/N-doped C composites benefit from its unique micro-polyhedrons hollow structure as well as the synergism of two kinds of electroactive materials and nitrogen-modified carbon material. First, the N-doped carbon matrix acted could effectively accommodate the volume changes and inhibited material structure damage during the Li ions conversion reaction. Second, the carbon-nitrogen surface modification increased the lithium storage position, promoted the wettability of the electrode and electrolyte, and improved the conductive properties of the electrode materials. In summary, the two-component reactive composite following carbon-nitrogen modification possessed better performance.

6. SUMMARY AND OUTLOOK

This study briefly reviewed the research progress involving the spinel structure ZnFe₂O₄ in lithium battery anode materials. ZnFe₂O₄ is demonstrated by its high theory capacity and lower cost as

electrode materials. However, its low electron conductivity, large volume expansion effect, poor cycle stability and rate performance limit its application and development. Multi-component ZnFe_2O_4 materials with special structures and morphologies were synthesized using different methods such as coating with different morphological carbon materials or compounding transition metal oxides. The ZnFe_2O_4 composite material was observed to enhance electrical conductivity, improve structural stability, and fully exert the synergistic stabilization effect of each structure and component, improving its electrochemical performance as an electrode material.

Furthermore, the material morphology was found to have a direct impact on electrochemical properties, and the initial morphology of the material dynamically changed during the cycling process. This considered as a key direction in material development research in regard to observing and obtaining changes in morphology throughout the entire process and studying the relationship between morphology, structure change and electrochemical performance. The improved electrochemical performance of two or more kinds of metal oxides has also garnered increasing attention. However, relatively few reports exist on multi-component metal oxide composites. Hence, it is necessary to further elucidate the influence of the composite mechanism and material structure on electrochemical performance. Due to the in-depth application of lithium batteries in power storage and new energy vehicles, the comprehensive electrochemical performance of electrode materials based on ZnFe_2O_4 materials requires further development in order to promote their application and development in anode materials for lithium batteries.

References

1. Q. Ran, H. Zhao, Q. Wang, X. Shu, Y. Hu, S. Hao, M. Wang, J. Liu, M. Zhang, H. Li, N. Liu, X. Liu, *Electrochim. Acta*, 299 (2019) 971-978.
2. H. Zhao, S. Liu, Z. Wang, Y. Cai, M. Tan, X. Liu, *Electrochim. Acta*, 199 (2016) 18-26.
3. M. Zhang, M. Tan, H. Zhao, S. Liu, X. Shu, Y. Hu, J. Liu, Q. Ran, H. Li, X. Liu, *Appl. Surf. Sci.*, 458 (2018) 111-118.
4. Q. Ran, H. Zhao, X. Shu, Y. Hu, S. Hao, Q. Shen, W. Liu, J. Liu, M. Zhang, H. Li, X. Liu, *ACS Appl. Energy Mater.*, 2 (2019) 3120-3130.
5. H. Zhao, J. Wang, G. Wang, S. Liu, M. Tan, X. Liu, S. Komarneni, *Ceram. Int.*, 43 (2017) 10585-10589.
6. Z. Zhang, X. Liu, Y. Wu, H. Zhao, *J. Solid State Electrochem.*, 19 (2014) 469-475.
7. H. Yue, Q. Wang, Z. Shi, C. Ma, Y. Ding, N. Huo, J. Zhang, S. Yang, *Electrochim. Acta*, 180 (2015) 622-628.
8. L. Yao, H. Deng, Q.-A. Huang, Q. Su, G. Du, *Ceram. Int.*, 43 (2017) 1022-1028.
9. H. Zhao, S. Liu, Z. Wang, Y. Cai, M. Tan, X. Liu, *Ceram. Int.*, 42 (2016) 13442-13448.
10. H. Zhao, S. Liu, X. Liu, M. Tan, Z. Wang, Y. Cai, S. Komarneni, *Ceram. Int.*, 42 (2016) 9319-9322.
11. H. Zhao, B. Chen, C. Cheng, W. Xiong, Z. Wang, Z. Zhang, L. Wang, X. Liu, *Ceram. Int.*, 41 (2015) 15266-15271.
12. H. Zhao, S. Liu, Y. Cai, Z. Wang, M. Tan, X. Liu, *J. Alloy. Compd.*, 671 (2016) 304-311.
13. Z. Zhang, X. Liu, Y. Wu, H. Zhao, B. Chen, W. Xiong, *J. Electrochem. Soc.*, 162 (2015) A737-A742.
14. Z. Zhang, X. Liu, L. Wang, Y. Wu, H. Zhao, B. Chen, *Solid State Ionics*, 276 (2015) 33-39.
15. M. Zhang, H. Zhao, M. Tan, J. Liu, Y. Hu, S. Liu, X. Shu, H. Li, Q. Ran, J. Cai, X. Liu, *J. Alloy.*

- Compd.*, 774 (2019) 82-92.
16. S. Goriparti, E. Miele, F. De Angelis, E. Di Fabrizio, R. Proietti Zaccaria, C. Capiglia, *J. Power Sources*, 257 (2014) 421-443.
 17. P. Poizot, S. Laruelle, S. Grugeon, D. L., T. J-M., *Nature*, 407 (2000) 496-499.
 18. W.-J. Zhang, *J. Power Sources*, 196 (2011) 13-24.
 19. X. Zhu, Y. Zhu, S. Murali, M.D. Stoller, R.S. Ruoff, *ACS Nano*, 5 (2011) 3333-3338.
 20. M.S. Park, G.X. Wang, Y.M. Kang, D. Wexler, S.X. Dou, H.K. Liu, *Angew Chem. Int. Ed.*, 46 (2007) 750-753.
 21. Y. Qu, D. Zhang, X. Wang, H. Qiu, T. Zhang, M. Zhang, G. Tian, H. Yue, S. Feng, G. Chen, *J. Alloy. Compd.*, 721 (2017) 697-704.
 22. J. Li, S. Xiong, Y. Liu, Z. Ju, Y. Qian, *ACS Appl. Mater. Inter.*, 5 (2013) 981-988.
 23. J. Yao, Y. Zhang, J. Yan, H. Bin, Y. Li, S. Xiao, *Mater. Res. Bull.*, 104 (2018) 188-193.
 24. Z. Yang, Y. Wan, G. Xiong, D. Li, Q. Li, C. Ma, R. Guo, H. Luo, *Mater. Res. Bull.*, 61 (2015) 292-297.
 25. H. Yang, X. Bai, P. Hao, J. Tian, Y. Bo, X. Wang, H. Liu, *Sensor. Actuat. B: Chem.*, 280 (2019) 34-40.
 26. L. Wu, T. Wu, M. Mao, M. Zhang, T. Wang, *Electrochim. Acta*, 194 (2016) 357-366.
 27. C. Wang, Y. Li, Y. Ruan, J. Jiang, Q.-H. Wu, *Mater. Today Energy*, 3 (2017) 1-8.
 28. R.M. Thankachan, M.M. Rahman, I. Sultana, A.M. Glushenkov, S. Thomas, N. Kalarikkal, Y. Chen, *J. Power Sources*, 282 (2015) 462-470.
 29. X. Tang, X. Hou, L. Yao, S. Hu, X. Liu, L. Xiang, *Mn-doped Mater. Res. Bull.*, 57 (2014) 127-134.
 30. S.J. Yang, S. Nam, T. Kim, J.H. Im, H. Jung, J.H. Kang, S. Wi, B. Park, C.R. Park, *J Am. Chem. Soc.*, 135 (2013) 7394-7397.
 31. J. Shi, X. Zhou, Y. Liu, Q. Su, J. Zhang, G. Du, *Mater. Res. Bull.*, 65 (2015) 204-209.
 32. P. Ren, Z. Wang, B. Liu, Y. Lu, Z. Jin, L. Zhang, L. Li, X. Li, C. Wang, *J. Alloy. Compd.*, 812 (2020).
 33. H. Qiao, Z. Xia, Y. Fei, L. Cai, R. Cui, Y. Cai, Q. Wei, Q. Yao, *Ceram. Int.*, 43 (2017) 2136-2142.
 34. H. Qiao, R. Li, Y. Yu, Z. Xia, L. Wang, Q. Wei, K. Chen, Q. Qiao, *Electrochim. Acta*, 273 (2018) 282-288.
 35. F. Mueller, D. Bresser, E. Paillard, M. Winter, S. Passerini, *J. Power Sources*, 236 (2013) 87-94.
 36. L. Lv, Y. Wang, P. Cheng, B. Zhang, F. Dang, L. Xu, *Sensor. Actuat. B: Chem.*, 297 (2019).
 37. X. Lu, A. Xie, Y. Zhang, H. Zhong, X. Xu, H. Liu, Q. Xie, *Electrochim. Acta*, 249 (2017) 79-88.
 38. J. Liu, The Effect of Calcination Temperature on Combustion *J. Electrochem. Sci.*, (2020) 1571-1580.
 39. M J Akhtar, M Nadeem, S Javaid, M Atif, *Journal of Physics: Condensed Matter*, 2009, 21(40): 405303.
 40. F PAPA, L PATRON, O CARP, C PARASCHIV, I BALINVT. *Rev. Roum. Chim*, 2010, 55(1): 33-38.
 41. L. Hou, R. Bao, D.k. Denis, X. Sun, J. Zhang, F.u. Zaman, C. Yuan, *Acta*, 306 (2019) 198-208.
 42. X. Guo, X. Lu, X. Fang, Y. Mao, Z. Wang, L. Chen, X. Xu, H. Yang, Y. Liu, *Electrochem. Commun.*, 12 (2010) 847-850.
 43. Y. Gao, L. Yin, S.J. Kim, H. Yang, I. Jeon, J.-P. Kim, S.Y. Jeong, H.W. Lee, C.R. Cho, *Electrochim. Acta*, 296 (2019) 565-574.
 44. F.M. Courtel, H. Duncan, Y. Abu-Lebdeh, I.J. Davidson, *J. Mater. Chem.*, 21 (2011).
 45. Y. Ding, Y. Yang, H. Shao, *Electrochim. Acta*, 56 (2011) 9433-9438.
 46. P.F. Teh, Y. Sharma, S.S. Pramana, M. Srinivasan, *J. Mater. Chem.*, 21 (2011).
 47. B. Wang, S. Li, B. Li, J. Liu, M. Yu, *New J. Chem.*, 39 (2015) 1725-1733.
 48. X.-B. Zhong, Z.-Z. Yang, H.-Y. Wang, L. Lu, B. Jin, M. Zha, Q.-C. Jiang, *J. Power Sources*, 306 (2016) 718-723.

49. L.-X. Liao, M. Wang, T. Fang, G.-P. Yin, X.-G. Zhou, S.-F. Lou, *J. Inorg. Mater.*, 31 (2016).
50. Q. Gan, K. Zhao, S. Liu, Z. He, *Electrochim. Acta*, 250 (2017) 292-301.
51. Y. L. Wang, L. X. Zhang, *J. Process. Eng.*, 15 (2015) 169-173.
52. C.T. Cherian, M.V. Reddy, G.V.S. Rao, C.H. Sow, B.V.R. Chowdari, *J. Solid State Electrochem.*, 16 (2012) 1823-1832.
53. D. Feng, H. Yang, X. Guo, *Chem. Eng. J.*, 355 (2019) 687-696.
54. K.-T. Chen, H.-Y. Chen, C.-J. Tsai, *Electrochim. Acta*, 319 (2019) 577-586.
55. J. Cai, C. Wu, Y. Zhu, P.K. Shen, K. Zhang, *Electrochim. Acta*, 187 (2016) 584-592.
56. H. Zhao, F. Li, X. Liu, W. Xiong, B. Chen, H. Shao, D. Que, Z. Zhang, Y. Wu, *Electrochim. Acta*, 166 (2015) 124-133.
57. Z. Xing, Z. Ju, J. Yang, H. Xu, Y. Qian, *Nano Res.*, 5 (2012) 477-485.
58. P.G. Bruce, B. Scrosati, J.M. Tarascon, *Angew Chem. Int. Ed.*, 47 (2008) 2930-2946.
59. J.M. Won, S.H. Choi, Y.J. Hong, Y.N. Ko, Y.C. Kang, *Sci. Rep.*, 4 (2014) 5857.
60. G. Gao, L. Shi, S. Lu, T. Gao, Z. Li, Y. Gao, S. Ding, *Dalton Trans.*, 47 (2018) 3521-3529.
61. W. Choi, I. Lahiri, R. Seelaboyina, Y.S. Kang, *Crit. Rev. Solid State*, 35 (2010) 52-71.
62. J. Sui, C. Zhang, D. Hong, J. Li, Q. Cheng, Z. Li, W. Cai, *J. Mater. Chem.*, 22 (2012).
63. Y. Dong, Y. Xia, Y.-S. Chui, C. Cao, J.A. Zapien, *J. Power Sources*, 275 (2015) 769-776.
64. Y. Wang, Y. Jin, R. Zhang, M. Jia, *Appl. Surf. Sci.*, 413 (2017) 50-55.
65. X. Gu, L. Chen, Z. Ju, H. Xu, J. Yang, Y. Qian, *Adv. Funct. Mater.*, 23 (2013) 4049-4056.
66. F. Zou, X. Hu, Z. Li, L. Qie, C. Hu, R. Zeng, Y. Jiang, Y. Huang, *Adv. Mater.*, 26 (2014) 6622-6628.
67. L. Hou, L. Lian, L. Zhang, G. Pang, C. Yuan, X. Zhang, *Adv. Funct. Mater.*, 25 (2015) 238-246.
68. Y. Ma, Y. Ma, D. Geiger, U. Kaiser, H. Zhang, G.-T. Kim, T. Diemant, R.J. Behm, A. Varzi, S. Passerini, *Nano Energy*, 42 (2017) 341-352

© 2020 The Authors. Published by ESG (www.electrochemsci.org). This article is an open access article distributed under the terms and conditions of the Creative Commons Attribution license (<http://creativecommons.org/licenses/by/4.0/>).